Efficient capture of circulating tumor cells with a novel immunocytochemical microfluidic device

Mary Nora Dickson,[1,2,a)] Pavel Tsinberg,[1] Zhongliang Tang,[1]
Farideh Z. Bischoff,[1] Timothy Wilson,[1] and Edward F. Leonard[2]
[1]*Biocept, Inc., 5810 Nancy Ridge Drive Suite 150, San Diego, California 92121, USA*
[2]*Columbia University School of Engineering and Applied Science, Department of Chemical Engineering, 801 Mudd, 500 W. 120th Street, New York, New York 10027, USA*

(Received 21 February 2011; accepted 19 July 2011; published online 22 August 2011)

Ability to perform cytogenetic interrogations on circulating tumor cells (CTCs) from the blood of cancer patients is vital for progressing toward targeted, individualized treatments. CTCs are rare compared to normal (bystander) blood cells, found in ratios as low as $1{:}10^9$. The most successful isolation techniques have been immunocytochemical technologies that label CTCs for separation based on unique surface antigens that distinguish them from normal bystander cells. The method discussed here utilizes biotin-tagged antibodies that bind selectively to CTCs. The antibodies are introduced into a suspension of blood cells intending that only CTCs will display surface biotin molecules. Next, the cell suspension is passed through a microfluidic channel that contains about 9000 transverse, streptavidin coated posts. A CTC making contact with a post has the opportunity to engage in a biotin-streptavidin reaction that immobilizes the cell. Bystander blood cells remain in suspension and pass through the channel. The goal of the present study is to establish the technical performance of these channels as a function of antigen density and operating conditions, especially flow rate. At 18 μL/min, over 70% of cells are captured at antigen densities greater than 30 000 sites/cell while 50% of cells are captured at antigen densities greater than 10 000. It is found that lower flow rates lead to decreasing cell capture probabilities, indicating that some streamlines develop which are never close enough to a post to allow cell-post contact. Future modeling and streamline studies using computational fluid dynamics software could aid in optimization of channel performance for capture of rare cells. © *2011 American Institute of Physics*. [doi:10.1063/1.3623748]

BACKGROUND

Physicians have long noted the presence of circulating tumor cells (CTCs) in the blood of cancer patients.[1] CTC detection plays an increasing role in cancer diagnosis, prognostication, and surveillance.[2–5] With the advent of individualized, targeted cancer therapies which depend on genetic analysis of tumor cells, a non-invasive and inexpensive platform for CTC capture and interrogation has become a necessity. In a blood sample containing approximately 10×10^9 healthy cells, there may be 1 to 1000 CTCs.[3] Thus, high-yield, high-purity isolation is difficult. The leading CTC isolation technologies have been reviewed[5–7] and two broad separation criteria—physical and immunocytochemical—can be seen to encompass the many approaches to the problem. Physical separation methods include filtration, addressing primarily cell size, and density gradient centrifugation, addressing the differences in density amongst cell types. Density gradient is commonly used as a pre-enrichment step where it may reduce the ratio of background blood cells to CTCs by several orders of magnitude, primarily by removing red blood

[a)]Author to whom correspondence should be addressed. Electronic mail: mary.dickson@gmail.com. Tel.: (414)807-1597.

cells (RBCs) and heavier white blood cells such as granulocytes. This paper will focus on immunocytochemical approaches with particular emphasis on a system developed in the authors' laboratory.

Immunocytochemical technologies exploit the selective binding of particular antibodies to surface antigens present on CTCs that are not present on bystander blood cells. Since association with an antibody does not, per se, render a cell separable, the antibody must be predisposed to participate in a subsequent separation process. Two approaches have been taken: either (1) the antibodies are admixed with the cell sample to bind to cells with complexation occurring throughout the suspending volume, in which case the complexes must subsequently be captured, or (2) cells are interrogated as they follow a directed flow path over antibody that has been immobilized onto a collecting surface.

The Veridex CellSearch® (the registered trade name of Veridex LLC, Raritan, NJ) system uses the first approach, introducing antibody-bearing magnetic particles ("ferrofluids") into the blood to search out and bind to CTCs.[8] The ferrofluid-CTC complexes are collected under an applied magnetic field onto the surface of a plate for quantification and recovery. Several studies indicate that CellSearch recovers CTCs from the blood of up to 70% of patients with metastatic breast and prostate cancer.[8,9] However, in one study, CellSearch only recovered CTCs from 20-40% patients with metastatic breast, ovarian, colorectal, lung, and other metastatic cancers.[3] Nevertheless, this product has shown success in predicting patient survival rates, and is serving as an important diagnostic tool for clinicians.[3,8–10] The Veridex method allows for different biotinylated antibodies to be used solely or in combination, allowing for the modulation of surface antibody density and offering flexibility in selecting different cell types.

The second method is exemplified by the "CTC-chip," a microfluidic device developed by the bio-MEMS Resource Center at Harvard Medical School, Boston, MA.[11] The CTC-chip platform is a microfluidic channel with 78 000 identical micron-scale, transverse posts ordered in a regular geometric array. These posts are coated with antibodies specific to a CTC surface antigen so that given sufficient contact, antibody-antigen reactions occur, binding CTCs to the interior surface of the chip. Suspended cells flow over the posts allowing for cell-post contact.[12] Published data report recovery of CTCs from up to 99% of metastatic lung, prostate, pancreatic, breast, and colon cancer patients, with captured CTCs at a purity level of 50%.[11]

Each method for isolating CTC's based on their surface antigens has its advantages and disadvantages. Ligating free antibodies gives an investigator, maximum choice of antibodies including "cocktails" with differently proportioned antibody components. Capturing with immobilized antibodies avoids the need for subsequent collection of ligated cells and allows for the choice of a desirable display of captured cells, allowing location and identification by staining with fluorescent secondary antibodies and subsequent analysis by fluorescence in-situ hybridization (FISH).[13–15] A combination of these two methods in which cells are captured onto a display surface via the use of biotinylated soluble antibodies using a channel labeled with streptavidin offers special advantages. Antibody selection and specification of the cocktail remains with each investigator, with biotinylation as the only extra step. Ligation time is controlled by the investigator and is not coupled to channel size and flowrates. The more difficult task of preparing the channel surface is left to the manufacturer who uses only one, standard capturing agent, streptavidin. The capture kinetics within the chamber vary principally with the number of antibodies associated with a cell and not the nature of the ligated antibody, since only the biotin-streptavidin reaction occurs during capture.

The rest of this paper takes an analytical and quantitative modeling approach to a novel technology of this type. This device, called Cell Enrichment and Extraction™ (CEE) channel, was developed in the authors' laboratories. It allows for a wide, investigator-driven choice of antibody or antibodies—a feature that may be crucial in obtaining comprehensive capture of heterogeneous cell populations. As described above, captured cells are displayed desirably for further investigations, such as FISH.

The technology calls for pre-enrichment of a blood sample using density centrifugation to remove RBCs. The enriched cell fraction is then incubated with biotin-labeled antibodies targeted toward specified CTCs. Next, a suspension of blood cells is drawn through a microfluidic

channel manufactured out of polydimethylsiloxane (PDMS), using standard soft lithography manufacturing techniques for microelectromechanical systems (MEMs) and the channel is bonded to a glass coverslip. The entire inner lumen of the covered channel (both the PDMS and glass coverslip) is derivitized with streptavidin, tethered to the PDMS via a long polyethylene glycol (PEG) chain.

The channel interior contains about 9000 transverse, randomly sized, randomly positioned posts, which are 75-150 μm in diameter. The distribution of post sizes, dimensions, and positions relative to each other have been optimized to minimize straight-line, regularized streamline flow, and thus to encourage frequent and unbiased collisions between posts and cells.[16] The total volume occupied by the posts is about 25% of the total volume of the channel. The channel itself holds 15 μl of fluid volume, discounting the volume of the inlet and outlet ports. While the density of posts in the channel could be higher, a minimum post separation was set at 70 μm in order prevent clogging when encountering cell clumps, debris, micro emboli, etc. The height of the channel is $\sim$55 μm, with posts spanning the entire height. All channels are exact replicates, which aids post capture analysis where captured cell positions are recorded.

Cells are seen to make contact with a post, slow, and roll around the post. Because the CTCs are coated with antibodies derivatized with biotin, which rapidly and nearly irreversibly binds to streptavidin, when a cocktail of biotinylated antibodies is used the number of possible sites of adhesion to a post per cell is increased because a common ligand pair (biotin/streptavidin) spans all antigen-antibody pairs of interest.

Cell capture can be conceptualized as the number of opportunities for capture afforded each cell in a sample, multiplied by the number of cells exposed, multiplied by the probability of each opportunity to result in actual capture. In flow fields seen in the CEE chamber (and as well in the CTC chip), a uniform flow field is established within an array that can be roughly defined as a number, R, of rows (each containing W posts spaced to span the width of the chamber). Cells zigzag, row-to-row. The opportunity for any one cell to be captured is then proportional to the number of rows, so long as wholesale bypassing of the posts is avoided. The number of cells exposed can be obtained as the product of cell concentration multiplied by the volume of suspension flowed through the chamber.

The most important and difficult component of cell capture to define and optimize is the local probability, k, of capture. This probability will be affected by antigen expression level on the particular cell, density of surface tethered recognition elements, streptavidin in this case, on the antibody, the antibody-antigen affinity constant and the flow conditions. Among similar cells and in fully developed (not row-dependent) flows, capture probability is likely to be independent of row number and to depend on geometry (post size and spacing) and flow-rate as well as the density and molecular configuration of ligands on the target cells and their molecular cognates affixed to the wetted surfaces of the chamber. Fast flows may inhibit capture by not providing sufficient time for reaction at any point along a cell's path and by exerting a shearing effect on partially ligated cells, but some fluid movement is necessary, and some inertial effects abetted by faster flows could improve capture.

Whatever the complex relationships defining the capture probability, it is experimentally measurable and the measured value provides a fundamental ruler with which to compare any of the different circumstances described above. Thus, we formally define k as the chance of capture as a cell passes each row of posts and n as the number of cells in suspension flowing past a given row. Therefore if n cells are in suspension flowing past a given row, the number of cells captured in that row is $k \times n$ where k is the probability of cell capture while passing a given row. The change in the number of cells left in suspension with respect to the number of rows passed is expressed

$$\frac{dn}{dr} = -k \times n$$

so that the number of cells captured in an arbitrary segment of channel is

$$\int -k \times ndr.$$

If n_0 is the number of cells flowing into a segment, it follows that the number of cells which are left in suspension after an arbitrary number of rows is

$$n = n_0 - \int k \times ndr.$$

This directly leads to an equation for n,

$$n = n_0 e^{-kr}.$$

This experiment calls for a count of the cells captured in distinct regions of r rows along the microchannel. This value n_{obs}, the complement of n is defined as

$$n_{cap} = n_0 - n_0 e^{-kr}.$$

This leads to an equation for the capture probability per row of a cell under a given condition in a channel segment of r rows

$$k = \frac{-\frac{\ln(n_0 - n_{cap})}{n_0}}{r}.$$

The k values are expected to remain constant, whence different k's observed for different channel segments may be indicative of unexpected flow effects or a change in the cell population, e.g., because the cells most likely to adhere are depleted, leaving a population which is then less adherent. Whether k values vary or remain constant, profiles of captured cells in a chamber in comparison to the exponential distribution expected for constant k permits assessing effects of local changes in flow and in adherence probability because of changes in the remaining cell population. These data may aid in improvement of channel design and may assist in the assessment of the labeled cell population.

MATERIALS AND METHODS

General protocol

Cell suspensions of buffy coat cells, CTCs or CTC proxies (Fig. 1: 1) are incubated with biotin-tagged antibody. (Fig. 1: 2) Next, a suspension of cells is drawn through the channel. Wherever a CTC makes contact with a post, the biotin on its surface reacts with streptavidin, thus immobilizing labeled cells. (Fig. 1: 3) Next, the captured cells are fluorescently stained (Fig. 1: 4) and counted using fluorescence microscopy (Fig. 1: 5). Modifications to this procedure allow for measurement of the effects of anti-clumping reagent (Fig. 1: 6) and bystander white blood cells (Fig. 1: 7), as done in Part I. An additional pre-labeling step allows for tumor cells to be incubated with multiple antibodies so cells selected according to different antigens can be simultaneously captured in one channel at a particular flow rate, as done in Part II (Fig. 1: 8). Cell lines, antibody preparation and microchannel set-up are identical for all experiments.

CEE microchannel manufacturing

CEE microchannels were manufactured in-house at Biocept, Inc. (San Diego, CA). A brief description of the process follows.

A negative mask is created from an epoxy resin (EPON SU-8), spun onto silicon wafer substrates as a 50 μm thick film of photoresist, and hardened by baking. A desired pattern is

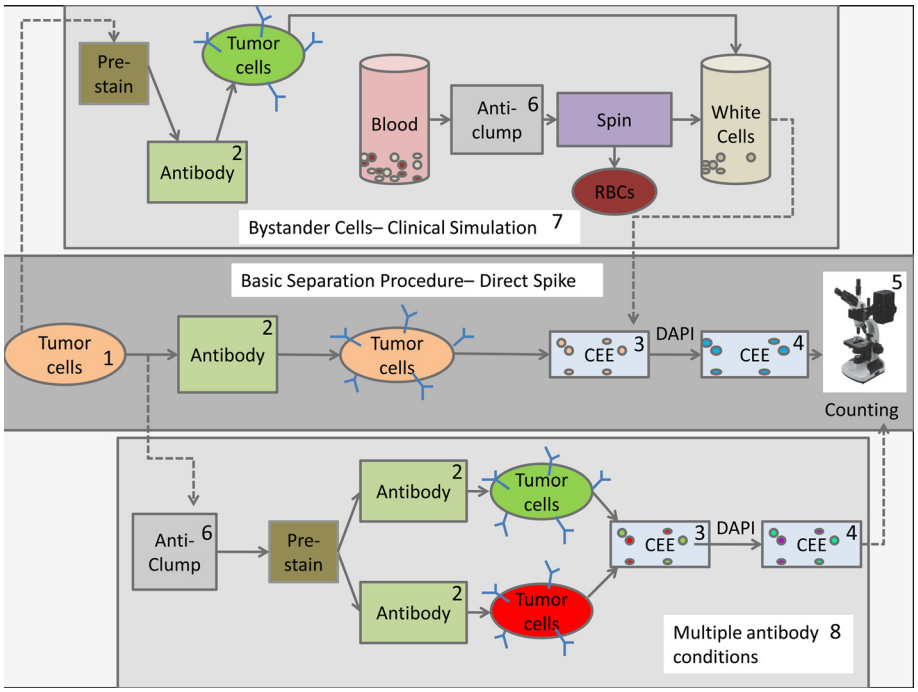

FIG. 1. General protocol. Tumor cells (Fig. 1: 1) are incubated with biotin-tagged antibody. (Fig. 1: 2) Next, a suspension of cells is drawn through the channel. Wherever a CTC makes contact with a post, the biotin on its surface reacts with streptavidin, thus immobilizing labeled cells. (Fig. 1: 3) Next, the captured cells are fluorescently stained (Fig. 1: 4) and counted using fluorescent microscopy (Fig. 1: 5). Modifications to this procedure allow for measurement of the effects of anti-clumping reagent (Fig. 1: 6) and bystander white blood cells (Fig. 1: 7), as done in Part I. An additional pre-labeling step allows for tumor cells incubated under multiple antibody conditions to be run simultaneously in one channel at a particular flow rate, as done in Part II (Fig. 1: 8). Cell lines, antibody preparation and microchannel set-up are identical for all experiments run.

exposed onto the photoresist through a Contact Mask Aligner. The exposed photoresist is developed in an SU-8 developer, a process which creates a negative-pattern mold that is then used as a master for replication of the channel geometry in PDMS. (Figure 2(a))

PDMS prepolymer and a curing agent (Sylgard 184 kit, Dow Corning) are mixed at a 10:1 ratio by weight. In order to avoid air bubble generation, the mixed polymer is first degassed in a vacuum chamber and then poured onto the master mold, which has been secured inside a molding cavity that also holds pins predetermining inlet and outlet ports. The PDMS is then cured at 90 °C and removed from the molding cavity.

The lumen of the channel is created by adhering the patterned face of the PDMS body to a glass coverslip after treatment of both surfaces with an oxygen plasma. A coverslip is used instead of a glass slide to enable high-resolution fluorescence microscopy. With coverslip thicknesses of 100 to 150 μm, magnifications up to 1000× (100× objective, plus a 10× eyepiece) are possible.

The assembled channels are then chemically derivitized with primary amines using aminosilane (3-aminopropyltriethoxysilane 99%, Aldrich). PEG is then attached to the amines through the NHS (*N*-hydroxysuccinimide) end of an NHS-PEG27-Maleimide linker. A thiolated streptavidin is then reacted to the maleimide end of the linker to finish the derivitization of the channel.

Microchannel set-up

For each experiment, four microchannels are run. A customized syringe pump which can provide flow through as many as 10 channels was designed at Biocept. Microchannels are attached to channel holding racks (also designed by Biocept) which maintain the channel angle

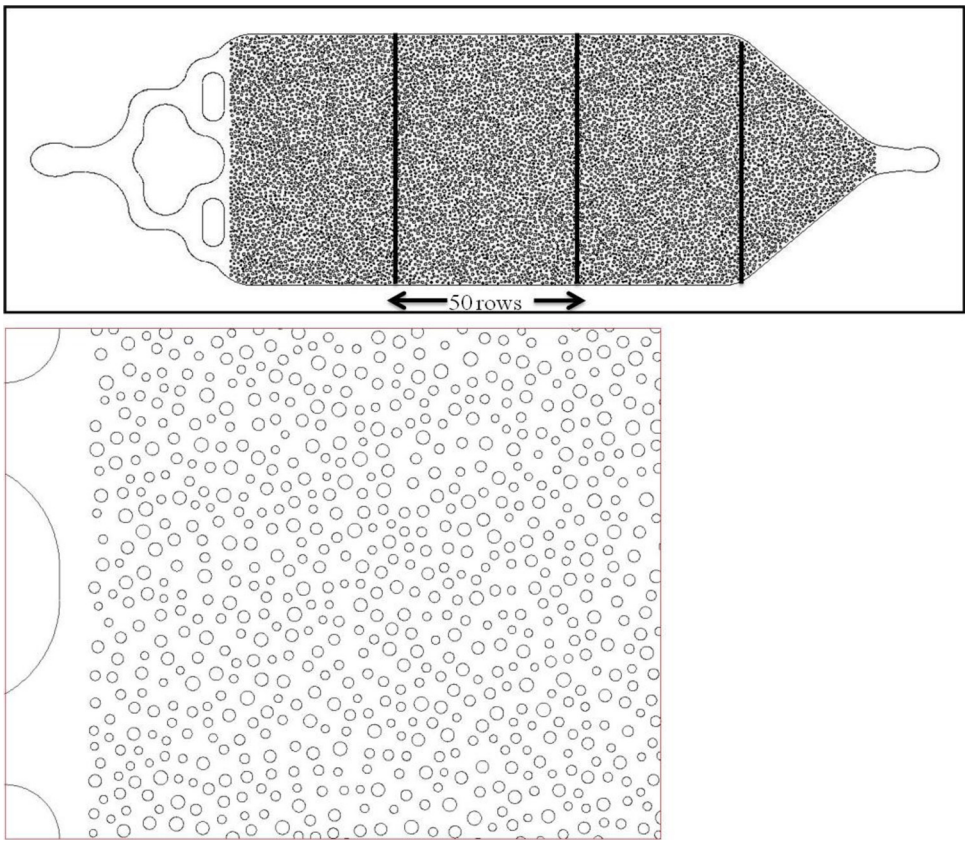

FIG. 2. Schematic of capture zones. (a) Close up of the channel.

at 45°. Each microchannel is connected to one of the pump's syringes via Teflon tubing. The 10 syringes are arranged radially around a central barrel which is locked, calibrated, and set to pull equally and simultaneously on all syringes. (see http://www.biocept.com/sites/default/files/CEET-Cell1.jpg) All reagents used in the cell capture and staining process are degassed in vacuum chambers at 27-29 in. Hg vacuum for 3-5 min. After microchannels are attached to their respective syringes, they are flushed twice with running buffer (PBS/BSA/EDTA) at high flow rates (150 μl/min).

Cancer cell lines

Standardized tumor cells are used as CTC proxies for most experiments. In order to eliminate day-to-day variability inherent in cell lines, a single batch of frozen SKOV (human ovarian cancer cells) (ATCC ID # SK-OV-3-IP1) are used to control for ovarian cells and normalized for expression of surface epithelial cell adhesion molecule (EpCAM). The cell line is grown according to standard in-house protocols, aliquoted into 50 000 cell pellets and kept frozen at −81 °C (Figure 1: 1).

Using fluorescence-activated cell sorting, (FACS) EpCAM expression was estimated to be 60 000 antigen molecules per cell. Measurement of EpCAM surface antigens was performed by incubating non-permeabilized SKOV cells with mouse anti-human EpCAM antibody, followed by incubation with PE-labeled anti-mouse IgG, according to standard flow cytometry protocol. After additional washes, to remove excess antibody, the cells were analyzed by flow cytometry. Flow cytometric estimation of antibodies bound per cell was determined by using BD QuantiBriteTM PE beads (BD Biosciences). By using known ratios of PE to antibodies, PE molecules per cell were converted to antibodies per cell.

SKOV cells are suspended in either fetal bovine serum (FBS) purchased from ATCC or media (as indicated in the procedures below) to yield suspensions of 2000-5000 cells/ml. The cells are incubated in serum overnight to mimic the clinical sample conditions.

Antibody preparation and incubation

To create cell samples with varying surface biotin density, cells are incubated in solutions of anti-EpCAM, composed of set ratios of biotinylated and non-biotinylated antibody (Figure 1: 2). Although selections of cell lines with different EpCAM expression were available, this approach was determined to be more repeatable and more controllable than attempting to vary either cell line or antibody.

To ensure that all binding sites are occupied, anti-epithelial cell adhesion molecule antibody (anti-EpCAM) 0.25mg/ml (T1; BD Biosciences, biotinylated in-house) is added in excess at a ratio of binding sites to antibodies of about 1:2000. Since biotin is small compared to the antibody (244 g/mol compared to 40 000 g/mol) we assume no difference in binding due to steric hindrance. Because the same antibody clone is used in both cases, and because the solution is incubated for sufficient time (greater than 30 min), we assume no kinetic difference in binding. These assumptions have been validated by flow cytometry, where both biotinylated and non-biotinylated versions of EpCAM antibody were titered on cell lines and showed no significant differences in binding. Thus, by controlling the percentage of antibodies which are biotinylated, the surface biotin density could be precisely manipulated. For the remainder of the paper, the result of this procedure will be referred to as "effective antigen density" which has units of biotinylated antibodies per cell.

Part I: Variable effective antigen densities

The first group of experiments described here seek to determine the correlation between capture efficiency and effective antigen density variation at a fixed channel flow rate.

Cell preparation

Direct spike experiment preparation

Untreated SKOV aliquots are suspended in RPMI-1640 medium purchased from ATCC (Manassas, VA) (Figure 1: 1-5). Cells are aliquoted into 1.7 ml Eppendorf tubes and each is incubated with an antibody solution as described above (Fig. 1: 2). The number of cells per μl is manually counted and a volume of cell suspension containing approximately 150 cells is calculated for each antibody solution. Aliquots of this volume are analyzed with the microchannel (Fig. 1: 3) and then by staining and microscopic visualization (Fig. 1: 4-5). These procedures are described in detail below.

Bystander cell experiment (clinical simulation) preparation

SKOV aliquots are thawed at 37 °C and added to a vacutainer containing FBS (Figure 1: 7). Anti-clumping reagent is added to this suspension at a concentration of 2 w/vol. %. Tumor cells pre-labeled with the cytosolic label Cell Trace Kit Green (Invitrogen; Eugene, Oregon) are subsequently aliquoted into 1.7 ml Eppendorf tubes and incubated with an antibody solution. For each microchannel, one Eppendorf tube containing approximately 150 labeled SKOV cells is used. The total number of input cells is confirmed for each antibody solution by counting the cells in an identical volume on a microscope slide.

Bystander cells are prepared from mononuclear cells (PBMC) using a Percoll density gradient method and Leucosep tubes (Greiner). Each Leucosep tube is pre-filled with Percoll Plus (GE Healthcare, UK) at a density of 1.083 g/ml (adjusted to normal saline levels) and stored at room temperature (RT). Each 10 ml blood sample is diluted three fold with a $1\times$ PBS/$1\times$ Casein/EDTA buffer and poured directly into a Leucosep tube and centrifuged. After separation, the upper layer (above the separation barrier) is recovered by decanting into a 50 ml

conical tube through a 70 μm cell strainer (BD). The decanted sample is washed and pelleted. Following supernatant aspiration using a vacuum wand, a 1 ml cell pellet is resuspended and incubated with antibody cocktail for 30 min at room temperature. The final 1 ml cell pellet is washed three more times with PBS/Casein/EDTA. Each wash step consists of a 400G 10 min centrifugation, followed by supernatant aspiration. The resulting 1 ml pellet is resuspended in $1 \times$ PBS and counted so that a volume corresponding to $\sim 10^7$ cells can be added to each Eppendorf tube containing an SKOV aliquot. These aliquots now contain about 25×10^6 WBCs and about150 tumor cells, which is approximately the ratio expected in a clinical sample. Next, aliquots are analyzed using the microchannel as described below.

Microchannel capture and staining

Each microchannel loading tip is filled with PBS/BSA/EDTA and the pump is switched on at a volumetric flow rate of 18 μl/min (Figure 1: 3-4). The desired aliquot is loaded into the tip of each channel and run continuously until the tip has been emptied, refilled with running buffer, and emptied again. A final rinse is done with $1 \times$ phosphate buffer solution (PBS) from Mediatech, Inc. (Manassas, VA).

Next, the cells are fixed in place by exposing them to Polyethylene glycol *N*-hydroxysuccinimide (PEG-NHS) protein crosslinker (Pierce. Rockford, IL) for 10 min followed by quenching in methanol (MeOH) buffer for an additional 10 min. The channel is then rinsed with $1 \times$ PBS to remove remaining MeOH. The cell nuclei are stained using 4′,6-diamidino-2-phenylindole (DAPI III) counterstain (Abbott Molecular Inc., Des Plaines, IL).

Microchannel enumeration and capture position

Each microchannel is scored on an Olympus Bx51 fluorescent microscope at $200 \times$ magnification using a DAPI filter (excitation/emission $\lambda = 350[\pm 50]/470[\pm 40]$ nm) to determine the number and location of cells captured (Figure 1: 5). For the bystander cell experiment, captured cells are confirmed to be green-labeled SKOVs by fluorescence visualization (excitation/emission $\lambda = 480[\pm 40]/631[\pm 23]$ nm). The capture position of a cell is recorded as lying in the inlet, outlet, or in one of 3 bulk capture zones (Figure 2).

Part II: Variable flow rates

The second group of experiments, described here, seek to determine the correlation between capture efficiency and one of 5 different channel flow rates.

Variable flow rate SKOV

Variable flow rate experiment set up

In these experiments two SKOV cell populations differing only in their concentration of biotinylated antibody are to be spiked together into each channel studied. SKOV cells are first diluted and divided into two tubes (Figure 1: 8). The cells in one tube are labeled green using Cell Trace Kit Green and those in the other tube, red, using Cell Trace Kit Red, both from Invitrogen (Eugene, Oregon). Next, the cells in each tube are incubated with a different concentration of biotinylated antibody. From each tube, volumes of suspension corresponding to a set number of cells is aliquoted. One of each of these aliquots is to be spiked into each CEE channel to be analyzed and visualized by the procedures described below. Thus, each channel will receive two distinguishable cell populations differing in biotinylated antibody density. Each channel thus yields information on two cell populations of known difference, each subjected to the same channel conditions.

Microchannel capture and staining

One pump containing four channels is run at each of the pre-determined flow rates (Figure 1: 3-4). Each microchannel loading tip is then filled with running buffer and the pump is switched on

at the desired running rate, and one of each aliquot is loaded into the tip of each channel. Microchannels are run continuously at the designated volumetric flow rate until the loading tip has been emptied, then twice refilled with buffer and emptied to rinse the channel. A final rinse is done with $1 \times$ PBS.

Fixing and staining procedures are as described in Part I.

Microchannel enumeration and capture position

Each microchannel is then scored on an Olympus Bx51 fluorescent microscope using a triple DAPI/red/green filter (excitation/emission $\lambda = 350[\pm 50]/470[\pm 40]$; $\lambda = 480[\pm 40]/631[\pm 23]$; and $\lambda = 460$ $[\pm 13]/535[\pm 50]$ nm light, respectively) in order to distinguish the green-labeled cells from the red-labeled cells (Figure 1: 5). Again, capture position is recorded according to whether the cell has been found in the inlet, outlet, or one of 3 bulk capture zones.

The results are, then, the number of cells counted (captured) in each of the three capture zones after the loading tip has been emptied. These data are analyzed along with the known number of cells delivered to the chamber.

RESULTS AND DISCUSSION

Capture efficiency, *C*

The simplest measure of performance for a CTC capture device is its yield of evaluable cells relative to the total number of CTCs or CTC surrogates with which the device has been challenged. This ratio is called capture efficiency,

$$C = \frac{n_{cap}}{n_0}.$$

While this measure is expected to be responsive to antigen loading and the appropriateness of operating conditions relative to the device' design, one expects predictable high efficiency that is robust against the presence of bystander cells and small variations in preparative technique and operating conditions. This is supported by Figure 3, which plots capture efficiencies against effective antigen density. Figure 3(a) compares trials with and without bystander cells. Figure 3(b), shows the variation of capture efficiency with flow rate. Both plots show high capture at antigen densities as low as 30 000, falling off rapidly as antigen density is decreased below 10 000. Capture efficiencies remain above 70% for effective antigen densities higher than 30 000, but drop to 50% at effective antigen densities of about 10 000.

Probability of capture, *k*

For ease of in situ inspection of cells under the microscope, it is desirable that they be captured and displayed with appropriate spacing, not overlapping in the field of view, but short enough to be efficiently scanned by the technician. Thus, an important characterization for a channel intended for in-situ inspection is the relationship between the number of rows of posts in a channel and the number of cells which adhere under specific conditions. The parameter k can be used to unambiguously compare data collected in various geometries at varying flows, and with different types and number per cell of binding moieties. In these experiments, each k value is assumed constant within each capture zone i ($i = 1, 2, 3$) (Fig. 4) and is calculated for each zone as follows:

$$k_i = -\left.\frac{\ln\left(\frac{n_{out}}{n_0}\right)}{r}\right|_i = \frac{\ln\left(1 - \frac{n_{cap,i}}{n_{0,i}}\right)}{r_i},$$

where r is the number of rows in the zone, n_{out} the number of cells that leave zone i, and n_0 the number of cells which enter that particular zone. The value of r is 50 for each zone.

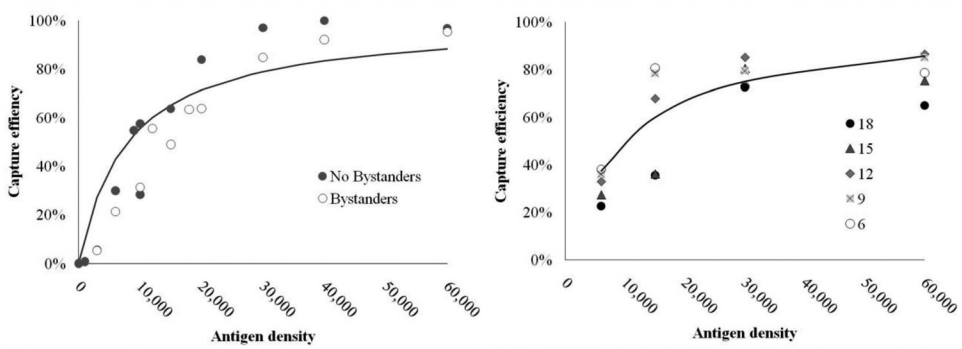

FIG. 3. Capture efficiency vs. antigen density.

Differences in adherence among cells entering a field of posts can depend upon cell properties. Without differences no useful distinction is made. Differences relevant to a cell's properties are useful while those depending upon the particular path that a cell follows are not. Thus, since many paths are possible, they should be identical. However, near a particular post in a field of posts the chance of adherence depends not only on the cell's "stickiness" but also on how the cell approaches the particular post.

Cells travel along streamlines that are well defined.[17] As seen in Figure 4, for a cell of a given diameter, perhaps 10 μm approaching a post whose diameter is about 10$\times$ larger, there are three possibilities: (i) a direct hit when the cell is on or near a streamline that points to the center of a post; or (ii) a glancing blow when the cell travels around the post but at some angle comes close enough to the post to adhere, or (iii) a total miss when the cell is on a streamline that does not bring the cell near enough to the post surface to allow adherence. If a cell passes many rows of posts and if the orientation of the cell relative to the posts does not depend upon how the cell passed an antecedent post, all cells should have, on average, the same chance of adherence, some sooner, some later, and some never if the number of rows is too small. In fact, the streamlines in an ordered bed of posts are regular and a cell on a streamline that bypasses a post in one row will be disposed to pass the next post it encounters. This consistent bypassing creates a difference for some cells that depends upon the particular path that these cells followed. It is possible for cells to move across streamlines but that is unlikely when cell concentrations and flow velocities are both low.

Both the Toner group[12,15] and the present authors have recognized this problem, the former by "staggering" the alignment of rows at intervals along the flow path and we by designing a bed in which, as noted above, the diameter and spacing of posts is randomized by a computer generation of the photolithographic mask that defines the bed. Computational fluid dynamic (CFD) studies, in progress, in the authors' laboratory indicate that randomization is more

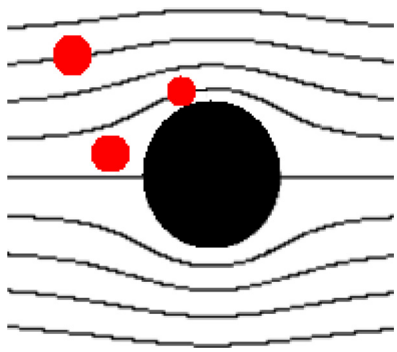

FIG. 4. Streamlines around post.

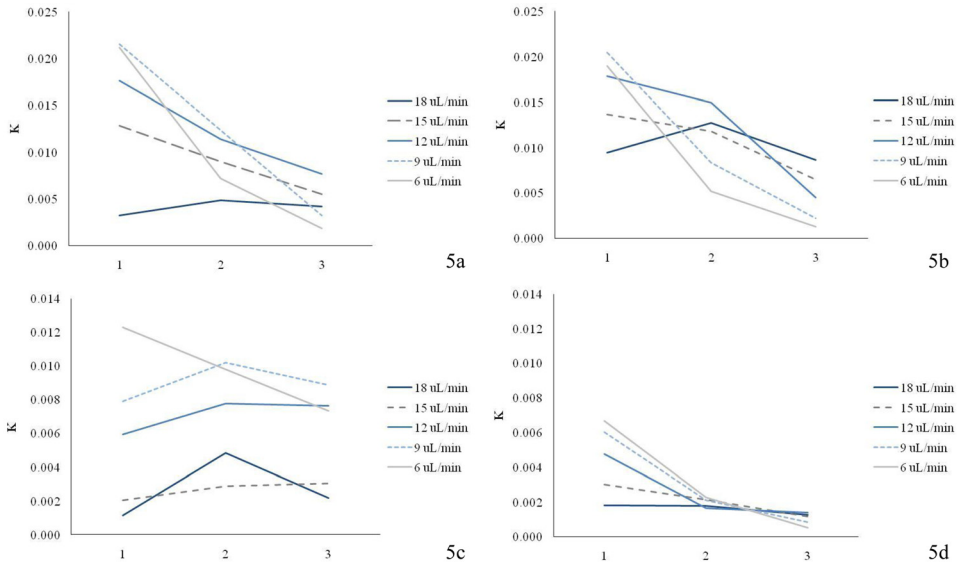

FIG. 5. k values vs. channel segment at various flow rates, plotted for four different effective antigen densities: (a) 60 000, (b) 30 000, (c) 15 000, and (d) 6000.

effective than staggering. The following results show the effect of varying flow rate and the effect of varying antigen density upon the capture efficiency.

Results obtained at different flow-rates

At each flow-rate, 6, 9, 12, 15, and 18 μl/min, k values are calculated for the three zones along the length of the channel. Decreasing k values indicate a decrease in capture probability as cells travel along the channel. Figure 5 displays the k values as calculated for each channel segment of SKOV populations with different effective antigen densities. The series represent various flow rates. In low flow-rate regimes, many of the k values decrease as cells travel along the channel. These charts show that for all antigen densities presented, excepting only 15 000, k values in low flow-rate regimes (6-15 μl/min) decrease as cells move through the channel. At the higher flow-rate of 18 μl/min antigen density does not change discernibly along the length of the channel. Figure 6 shows k values as calculated for each flow rate of SKOV populations with different effective antigen densities. Each channel zone is represented. The entrances of channels in low flow-rate regimes have high k values, while the k values at faster flow rates are lower and remain constant throughout the channel segments.

The maximum flow rate of 18 μl/min was determined from previous experiments with K562, SKOV, and T24 cell lines. K562 were tested with Gly-A, which is over-expressed on these cells to the order of 1×10^6 antigens per cells. Figure 7(a) shows how capture varies with flow rate in that cell line, where maximum capture is achieved between 12 and 24 μl/min. The relationship is similar for SKOV cells with EpCAM, Figure 7(b), but changes drastically for low-expressing T24 cells with EpCAM, Figure 7(c).

Figure 8 shows the capture of SKOV and SKBR cells with T2 antigen. Cells not fixed to the posts after capture can be removed from the channel by increasing flow rates. More experiments need to be done, however, to fully understand the relationship between antigen expression and shear rates.

Variable antigen density results

All experiments are run at 18 μl/min and trials are run with and without bystander cells as presented in Figures 9(a) and 9(b), in which are shown plots k values for different effective antigen densities, for each channel segment. These data show that k values remain constant

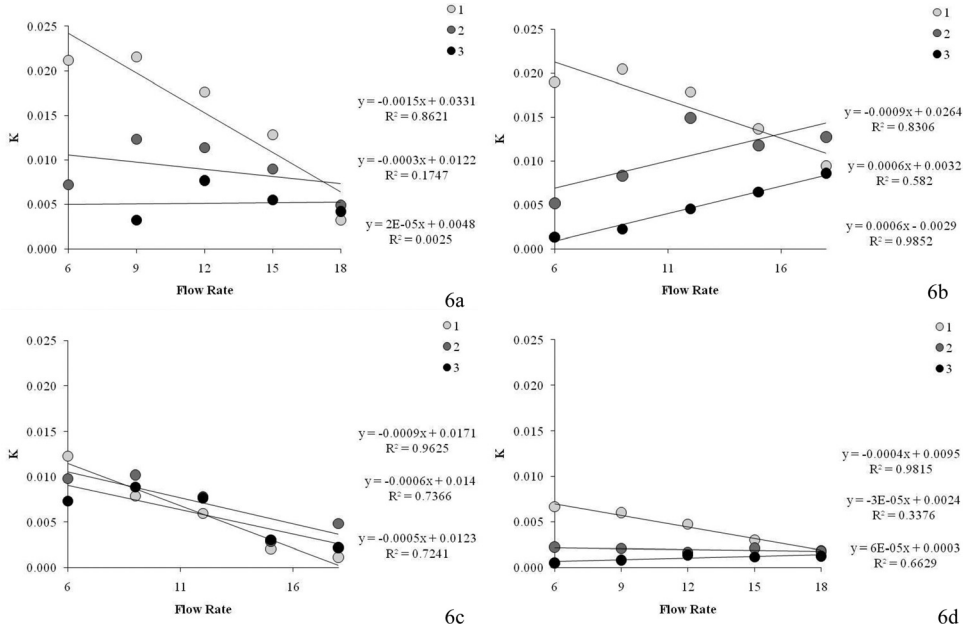

FIG. 6. *k* values vs. flow rate of various channel segments, plotted for four different effective antigen densities: (a) 60 000 (b) 30 000 (c) 15 000, and (d) 6000.

along the length of the channel as also observed in variable flow rate experiments. The results show a linear dependence of antigen density upon *k* as well.

The *k* value dependence on antigen density is likely caused by two effects. First, the chance of a biotin-streptavidin reaction scales with the number of surface ligands per cell. Also, the strength of the cell-post bond should be directly proportional to the number of ligand adhesions occurring as the cell moves past the post, and so should be the force opposing any shear effect. While it is outside the scope of this experiment to untangle the relative importance of these two effects, knowledge of the linear effect of antigen density on capture probability is valuable in determining ideal performance parameters.

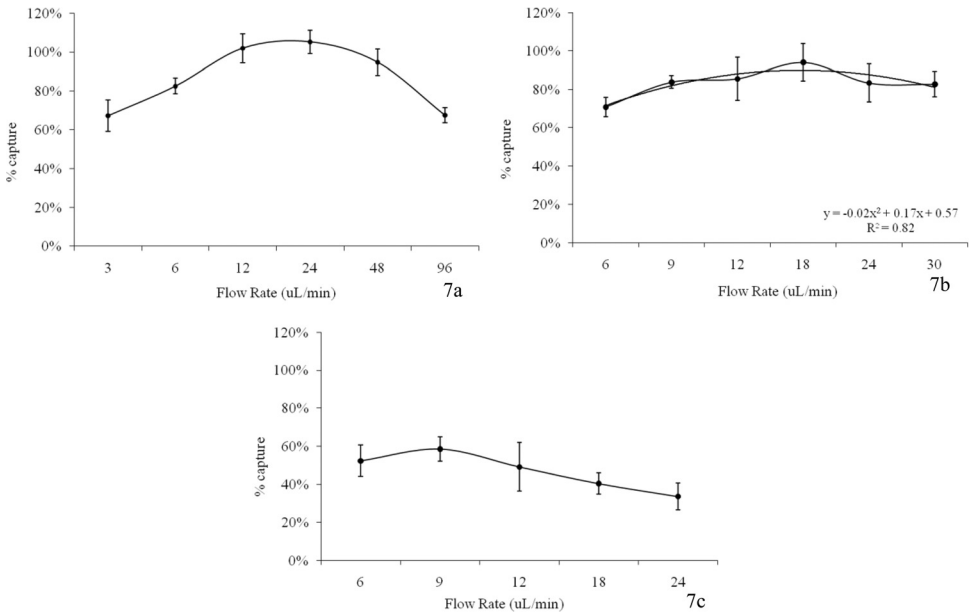

FIG. 7. Impact of flow rates upon percent of cells captured in: (a) K562 cells, (b) SKOV cells, and (c) T24cells.

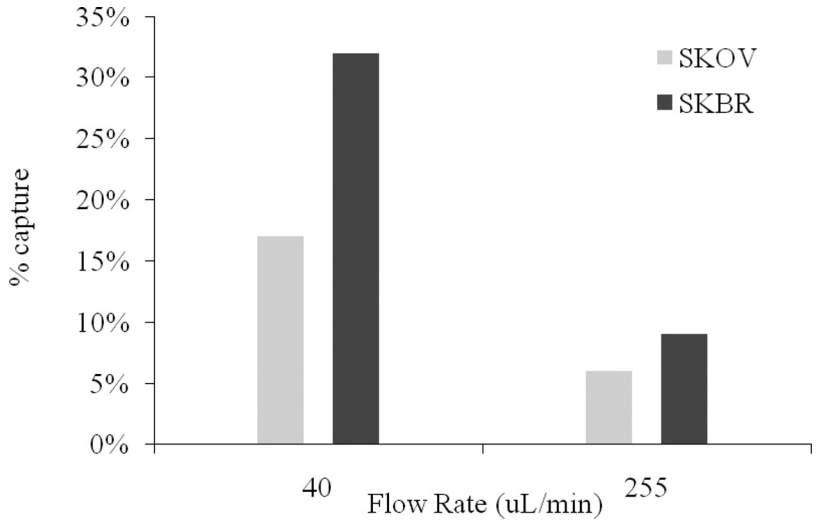

FIG. 8. Effect of high flow rate on percentage of SKOV and SKBR cells captured.

Bystander cells' effects on cell binding

As seen in Figure 9, at the bystander cell concentration studied here and at 18 μl/min, the k values appear to be only slightly lower than the in the control group. Due to the limited studies done with bystander cells, it is difficult to draw general conclusions about how they affect capture efficiency, but they could have contradictory effects: displacing tumor cells from posts, or forcing tumor cells off streamlines and into posts. Further studies would surely be of value.

Figure 10, which plots concentration of bystander cells against capture of SKOV cells, shows no significant variation.

Decreasing *k* values

If each cell is identical and if each cell is exposed to identical conditions as it zigzags from row to row, the expectation is that the probability of capture will remain constant along the channel. Therefore, the decrease in k observed in most trials indicates heterogeneity. The cell population may be heterogeneous in morphology or surface biotin presentation, or there may be variations in the contact of cells with posts, described above. Both are heterogeneities that cause disposed cells to adhere first, leaving a constantly less disposed population for subsequent adherence, manifesting thus a decreasing k. Different intrinsic tendencies to adhere can be distinguished from bypassing, an extrinsic phenomenon, by how k varies with flow conditions.

As argued above a decrease in k with distance is expected and seen in all cases. The data of Figure 6 add to this view. For cells with high antigen density, the largest k value variation from segment to segment is seen in low flow rate regimes, while there is very little variation at

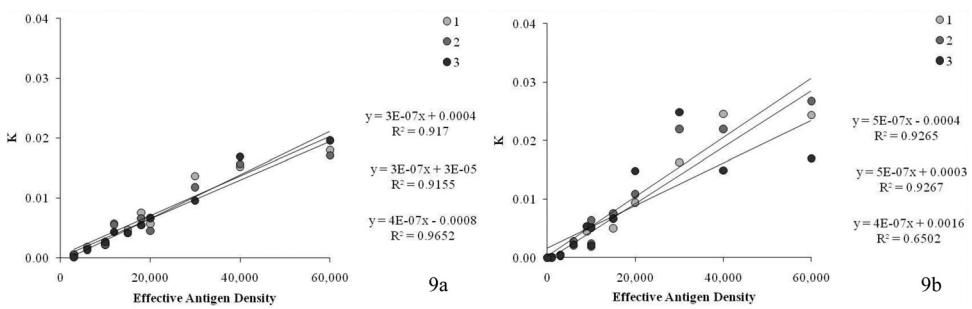

FIG. 9. k value vs. effective antigen density of various channel segments, (a) with and (b) without bystander cells.

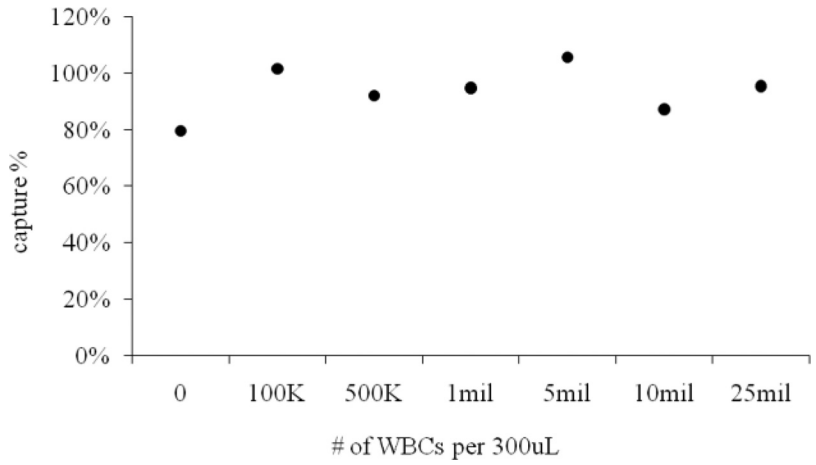

FIG. 10. Percent of cells captured as a function of bystander cell concentration.

high flow rates. As Figures 3(a) and 3(b) show, sensitivity of capture to the density of biotin-labeled antigen is low beyond values of 30 000, which indicates that bypassing may, by default, be the dominant effect that decreases k with increasing distance down the channel.

On the other hand, Figure 6 shows that k values of low antigen density cells do not vary significantly from segment to segment, no matter the flow rate. As can be seen from Figures 3(a) and 3(b), at low antigen densities, small differences have a large effect on capture. Therefore, the decrease in k along the channel is likely due to heterogeneity of cell populations in this regime.

Whole blood experiments

While preliminary processing of a blood sample by density gradient separation may engender the loss of some smaller or otherwise physically atypical CTC's, the processing of whole blood requires a much larger number of cells to be examined for each antigen-positive CTC that is captured. Gradient-separated cells occupy less than 1 ml. In contrast, the original sample volume of 8-10 ml would require a 7-9 h capture time at the 18 μl/min flowrate discussed in this paper, or a considerably larger capture device, with a concomitant increase in the amount and cost of post-capture reagents. Preliminary experiments with high-expression cells (SKBR) and low-expression (SKOV) cells showed high capture only with the former when the antibody was attached to the chamber, but high capture for both types when ligation with soluble biotinylated antibody was followed by capture in a streptavidin-bearing chamber. Data with actual CTC's are needed.

CONCLUSION

Overall, these data conclude that the CEE system conforms to simple physical principles and that it robustly and efficiently captures tumor cells under a variety of operating conditions. The calculation of capture probabilities allows the authors to make conclusions about the optimal running conditions as well as to make predictions about the likely capture efficiency of cells given their antigen density.

It appears that there should be a balance between the dominance of cells which follow non-contact streamlines, as seen at low flow-rates and the dominance of the obstacles to cell-post binding (such as shear and cell-post contact-time) that are seen at high flow-rates. In the CEE system, maximum consistent capture probability was seen at a flow-rate of 18 μl/min.

A detailed study of streamlines and subsequently of cell motion relative to these streamlines would aid in design and analysis of cell-capturing channels. Streamline prediction is well within the grasp of computational fluid dynamics and is underway in the authors' laboratories.

These data seem susceptible to combination with established theories that represent cell-cell interactions at higher cell concentrations, and so-called "lift" phenomena that illustrate the tendencies for cells near surfaces to cross streamlines. Actual binding reactions and their dependence on local shear and time have been developed for intravascular phenomena and give a starting point for perfecting models of cell capture in vitro.

While we will have limited knowledge of CTC antigen densities and of the biophysical behavior of endogenous CTC's, knowing how the flow parameters studied here affect capture over a wide range of antigen levels provides basic information of utility to anyone hoping to make a better microfluidic cell-capture system.

There is a clear two step recommendation. First, clinicians should employ antibody cocktails with a common capture principle, here biotin, in order to maximize relevant cell capture.[18] Second, while the data presented here show that in most cases with sufficient surface antibody density, greater than 70% capture was achieved, a channel design which forces variations in flow velocities along the channel length may overcome potential inefficiencies in capture seen at low antigen densities.

[1]L. A. Liotta, J. Kleinerman, and G. M. Saidel, Cancer Research **34**, 997 (1974), http://cancerres.aacrjournals.org/content/34/5/997.
[2]E. Racila, D. Euhus, A. J. Weiss, C. Rao, J. McConnell, L. W. M. M. Terstappen, and J. W. Uhr, Proc. Natl. Acad. Sci., USA **95**, 4589 (1998).
[3]W. J. Allard, J. Matera, M. C. Miller, M. Repollet, M. C. Connelly, C. Rao, A. G. J. Tibbe, J. W. Uhr, and L. W. M. M. Terstappen, Clin. Cancer Res. **10**, 6897 (2004).
[4]S. Meng, D. Tripathy, E. P. Frenkel, S. Shete, E. Z. Naftalis, J. F. Huth, P. D. Beitsch, M. Leitch, S. Hoover, D. Euhus, B. Haley, L. Morrison, T. P. Fleming, D. Herlyn, L. W. M. M. Terstappen, T. Fehm, T. F. Tucker, N. Lane, and J. Wang, Clin. Cancer Res. **10**, 8152 (2004).
[5]K. Pantel, R. H. Brakenhoff, and B. Brandt, Nat. Rev. Cancer **8**, 329 (2008).
[6]T. M. Scholtens, L. W. M. M. Terstappen, and A. G. J. Tibbe, U.S. Patent 7,666,308 B2 (2010).
[7]S. Nagrath, L. V. Sequist, S. Maheswaran, D. W. Bell, D. Irimia, L. Ulkus, M. R. Smith, E. L. Kwak, S. Digumarthy, A. Muzikansky, P. Ryan, U. J. Balis, R. G. Tompkins, D. A. Haber, and M. Toner, Nature **450**, 1235 (2007).
[8]S. Riethdorf, H. Fritsche, V. Muller, T. Rau, C. Schindlbeck, B. Rack, W. Janni, C. Coith, K. Beck, F. Janicke, S. Jackson, T. Gomet, M. Cristofanilli, and K. Pantel, Clinical Cancer Res. **13**(3), 920 (2007).
[9]D. C. Danila, G. Heller, G. A. Gignac, R. Gonzalez-Espinoza, A. Anand, E. Tanaka, H. Lilja, L. Schwartz, S. Larson, M. Fleisher, and H. I. Scher, Clin. Cancer Res. **13**(23), 7053 (2007).
[10]S. J. Cohen, C. J. A. Punt, N. Iannotti, B. H. Saidman, K. D. Sabbath, N. Y. Gabrail, J. Picus, M. Morse, E. Mitchell, M. C. Miller, G. V. Doyle, H. Tissing, L. W. M. M. Terstappen, and N. J. Meropol, J. Clin. Oncol. **26**(19), 3213 (2008).
[11]J. S. de Bono, H. I. Scher, R. B. Montgomery, C. Parker, M. C. Miller, H. Tissing, G. V. Doyle, L. W. W. M. Terstappen, K. J. Pienta, and D. Raghavan, Clin. Cancer Res. **14**(19), 6302 (2008).
[12]L. V. Sequist, S. Nagrath, M. Toner, D. Haber, and T. J. Lynch, J. Thorac. Oncol. **4**(3), 281 (2009).
[13]B. C. Handy, Biomarkers Med. **4**(1), 129 (2010).
[14]S. Maheswaran, L. V. Sequist, S. Nagrath, L. Ulkus, B. Brannigan, C. V. Collura, E. Inserra, S. Diederichs, A. J. Iafrate, D. W. Bell, S. Digumarthy, A. Muzikansky, D. Irimia, J. Settleman, R. G. Tompkins, T. J. Lynch, M. Toner, and D. Haber, N. Engl. J. Med. **359**, 366 (2008).
[15]R. J. Lee, S. L. Stott, S. Nagrath, L. E. Ulkus, D. M. Dahl, M. R. Smith, M. Toner, S. Maheswaran, and D. A. Haber, J. Clin. Oncol. (2009), http://www.asco.org/ascov2/Meetings/Abstracts&vmview=abst_detail_view&confID=65&abstractID=35729.
[16]P. Tsinberg and Z. Tang, U.S. Patent 7,695,956 B2 (2010).
[17]A. A. Adams, P. I. Okagbare, J. Feng, M. L. Hupert, D. Patterson, J. Gttert, R. L. McCarley, D. Nikitopoulos, M. C. Murphy, and S. A. Soper, J. Am. Chem. Soc. **130**(27), 8633 (2008).
[18]S. D. Mikolajczyk, L. S. Millar, P. Tsinberg, S. M. Coutts, M. Zomorrodi, T. Pham, F. Z. Bischoff, and T. J. Pircher, J. Oncol. **2011**, 252361 (2011).